12-1999

A Simplified Model of Wound Healing - II: The Critical Size Defect in Two Dimensions

J. S. Arnold
Old Dominion University

John A. Adam
Old Dominion University, jadam@odu.edu

Original Publication Citation

Arnold, J. S., & Adam, J. A. (1999). A simplified model of wound healing - II: The critical size defect in two dimensions. *Mathematical and Computer Modelling*, *30*(11-12), 47-60. doi:10.1016/s0895-7177(99)00197-1

PERGAMON Mathematical and Computer Modelling 30 (1999) 47–60

MATHEMATICAL AND COMPUTER MODELLING

www.elsevier.nl/locate/mcm

A Simplified Model of Wound Healing II: The Critical Size Defect in Two Dimensions

J. S. ARNOLD AND J. A. ADAM
Department of Mathematics and Statistics
Old Dominion University, Norfolk, VA 23529, U.S.A.

(Received and accepted July 1999)

Abstract—Recently, a one-dimensional model was developed which gives a reasonable explanation for the existence of a Critical Size Defect (CSD) in certain animals [1]. In this paper, we examine the more realistic two-dimensional model of a circular wound of uniform depth to see what modifications are to be found, as compared with the one-dimensional model, in studying the CSD phenomenon. It transpires that the range of CSD sizes for a reasonable estimate of parameter values is 1 mm–1 cm. More realistic estimates await the appropriate experimental data.

Keywords—Wound healing, Bone regeneration, Critical size defect, Growth factors, Diffusion equation.

INTRODUCTION

This paper is an attempt to construct a simple two-dimensional mathematical model of wound healing or tissue regeneration. This extends earlier work [1] to more realistic circular geometry, i.e., the cases of both a circular gouge and the entire removal of a circular portion of bone, and a circular gouge with some bone left in the wound area.

The time-development of the wound is not addressed here, we examine the conditions (e.g., wound size) under which tissue regeneration occurs. The primary objective is to find in each case a critical radius beyond which no healing occurs—the definition of a CSD.

The first model examined corresponds to a circular cylinder (with depth equal to the bone thickness) of bone being removed, so that no bone tissue remains in the vacated area. The second model allows some bone to remain in the excavated area, i.e., the cylinder thickness is less than that of the bone, (this is what is termed a gouge).

In each model we will assume, following [1], the existence of a thin ring of width δ which influences the mitotic activity up to the wound edge. In the models that follow, $C(r,t)$ will represent the concentration of a generic growth stimulator, where $0 \leq r \leq R$, R being the wound radius, and t being time, both in appropriate units.

THE NORMAL WOUND HEALING PROCESS

Bone is one of the tissues of the body capable of repairing itself. The process of bone healing involves new growth of cartilage-like cells called a sleeve, formed on the outer surface of the wound.

0895-7177/1999/$ - see front matter
PII: S0895-7177(99)00197-1

This usually occurs during the first few days after a wound has occurred. The gap between the sleeve of new bone is invaded by embryonic tissue which forms a bridge of connective tissue. This generally takes seven to ten days. The third stage of bone regeneration is the hardening or calcification of the fibrocartilage. This begins at the wound edge and moves toward the center. This usually occurs three to four weeks after the wound's birth. The next stage is calcification. During this stage the vascular system penetrates the fibrocartilage which causes it to be broken down and absorbed while the area is now replaced with a fiber bone. This takes place during the sixth to eighth week. Finally, the newly formed fiber bone is gradually changed to a rigid bone and eventually to normal bone within two months to two years. In nonunions, the calcification process fails to occur leaving the gap with fibrous tissue or fibrocartilage [2].

SUMMARY OF THE 1-D MODEL

The first model corresponds to bone (or indeed soft tissue) removed from an infinite plane, in which only a thin band of tissue at the wound edges takes part in regeneration. The edges are represented by $x = \pm L/2$. The region $[0, L/2]$ represents the right half of the wound where no tissue or bone remains, and $[L/2, L/2 + \delta]$ represents the layer creating the Growth Factor (GF) concentration. The governing differential equation is

$$\frac{\partial C}{\partial t} - D\frac{\partial^2 C}{\partial x^2} + \lambda C = PS(x),$$

in [1] where the parameters D, λ, and P, and the source term S are defined below for the present problem. It was found that for $C(L/2) \geq \theta$, $\delta \geq \delta_c = \alpha^{-1} ln(n/(n-1))$ with domain $n \geq 1$, where the parameter n is determined by P, λ, and θ. Clearly, δ_c is a lower bound for the GF active region.

In the second model, where it is assumed some bone remains in the wound area $[0, L/2]$, $C(L/2) \geq \theta$ produces a critical length, L_c, where $L_c = \alpha^{-1} ln((N(\delta))/(2 - N(\delta))$ where $N(\delta) = n[1 - e^{-\alpha\delta}]$. For further details see [1].

PARAMETER ESTIMATES

Some reasonable values for the parameters P, λ, and θ were found in [1] to be as follows: $\lambda = 1.6 \times 10^{-5}\ \text{sec}^{-1}$ (based on [3,4] work that the estimated half-life of chemical decay is about 12 hours; thus, $\lambda = (\ln 2)/12\,\text{hr}^{-1}$ which yields the preceding value). An approximate value for D, the diffusion parameter is $D \approx 5 \times 10^{-7}\,\text{cm}^2\ \text{sec}^{-1}$ which gives $\alpha \approx 6\,\text{cm}^{-1}$. The most difficult parameter to access is P/θ. A reasonable estimate is $P/\theta > 1.6 \times 10^{-5}\ \text{sec}^{-1}$ [1].

BASIC CONFIGURATIONS: MODEL I

We position the center of the circle at the origin. A wound disk of radius R is removed. As indicated earlier, we suppose that a generic "growth factor" (GF) is produced as a result of the trauma to the system, and it is the distribution of this growth factor that determines whether or not wound healing occurs in this model.

The differential equation describing the space and time distribution of the growth factor concentration $C(r, t)$ is

$$-\frac{D}{r}\frac{d}{dr}\left(r\frac{dC}{dr}\right) + \lambda C = PS(r) \tag{1}$$

where D, λ, and P are, respectively, the diffusion coefficient for the GF in the tissue, the decay or depletion rate of the GF, and the production rate of GF by the enhanced mitotically active cells in the vicinity of the wound edges. These are assumed to be constant in both models. Furthermore, $S(r)$ is the source term describing the distribution of GF production throughout the active tissue. In both models this is assumed to be uniform; thus,

$$S(r) = 1, \qquad \text{for } R \le r \le R + \delta,$$
$$S(r) = 0, \qquad \text{elsewhere,}$$

δ being the width of the active layer.

In equation (1), the time rate of change of GF concentration is not included because we are invoking the diffusive equilibrium approximation; full details and the justification for this can be found in [1]. The second term describes the spatial change due to diffusion, and the third term is the depletion or decay rate of GF as it interacts with the system as a whole, and is changed or removed.

MODEL I: EQUATIONS AND SOLUTIONS

If $\alpha^2 = \lambda/D$, then equation (1) can be written as

$$\frac{d^2C(r)}{dr^2} + \frac{1}{r}\frac{dC(r)}{dr} - \alpha^2 C(r) = \frac{-P}{S}S(r). \tag{2}$$

The boundary conditions are

- $C(r)$ and $(dC(r))/(dr)$ are both continuous at $\mathbf{R} + \delta$,
- $\lim_{r\to\infty} C(r) = 0$,
- $(dC(r))/(dr) = 0$ at $r = R$.

The first two conditions are obvious requirements. The third condition implies that there is no flux (number of molecules crossing unit area in unit time) at the wound edge. The second model will modify this restriction as we will permit tissue in the wound area capable of dispersing GF.

In terms of the dimensionless variable $x = \alpha r$, equation (2) becomes

$$x^2\frac{d^2C(x)}{dx^2} + x\frac{dC(x)}{dx} - x^2C(x) = \frac{-P}{D}S\left(\frac{x}{\alpha}\right). \tag{3}$$

The homogeneous solutions are modified Bessel functions of order zero. After some algebra, the solution can be written as

$$C(r) = \frac{-PK_1(\alpha(R+\delta))}{\lambda\beta_\delta}I_0(\alpha r) + \frac{-PK_1(\alpha(R+\delta))}{\lambda\beta_\delta}\frac{I_1(\alpha R)}{K_1(\alpha R)}K_0(\alpha r) + \frac{P}{\lambda}, \tag{4}$$

for $R \le r \le R + \delta$

$$C(r) = \left[\frac{-PK_1(\alpha(R+\delta))}{\lambda\beta_\delta}\frac{I_1(\alpha R)}{K_1(\alpha R)} + \frac{PI_1(\alpha(R+\delta))}{\lambda\beta_\delta}\right]K_0(\alpha r), \tag{5}$$

for $r > R + \delta$ where $\beta_\delta = (I_0K_1 + K_0I_1)(\alpha(R + \delta))$.

For the parameter values P, $\lambda = 1$, $\alpha R = 2$, and $\alpha\delta = .5$ the graph of $C(r)$ can be seen in Figure 1.

Using equation (4), we apply the criterion that

$$C(R) \ge \theta,$$

where θ represents a threshold value above which wound healing will occur for values of r satisfying this condition. The resulting equation is

$$\frac{P}{\lambda}\left\{1 - \frac{K_1(\alpha(R+\delta))}{\beta_\delta}\left[I_0(\alpha R) + \frac{I_1(\alpha R)K_0(\alpha R)}{K_1(\alpha R)}\right]\right\} \ge \theta \tag{6}$$

using standard identities for the [5], the second term in equation (6) simplifies to

$$\frac{K_1(\alpha R + \alpha\delta)(\alpha R + \alpha\delta)}{\alpha R K_1(\alpha R)} = Q(\alpha\delta). \tag{7}$$

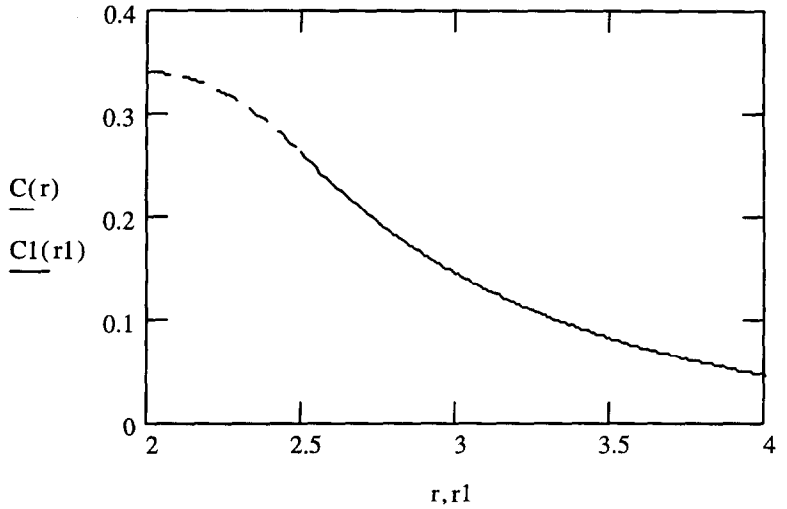

Figure 1. The growth factor concentration $C(r)$ for Model I, which assumes no bone is left in the wound area, $r \leq R$, where R is the radius size of the circular wound. $r1 = r$ for r in $[R + \delta, \infty]$. For illustrative purposes, the parameters P and $\lambda = 1$, and $\alpha\delta = .5$.

If $\alpha R = y$ and $\alpha\delta = \varepsilon$, then equation (7) can be written as

$$Q(\varepsilon) = \frac{K_1(y+\varepsilon)(y+\varepsilon)}{yK_1(y)} \leq 1 - \frac{\lambda\theta}{P} = 1 - \frac{1}{n}, \tag{8}$$

where $n = (P)/(\lambda\theta)$. We examine equation (7) as a function of $\varepsilon = \alpha\delta$, from which we can find a lower bound δ_c (δ critical) for the width δ above which healing can occur. It is not possible to obtain an explicit expression for δ_c in general, but if δ is small compared with R, then we may use first-order Taylor polynomials to simplify the Bessel functions. Thus, to first order in ε,

$$K_1(y+\varepsilon) \approx K_1(y) + \varepsilon K_1'(y).$$

Also,

$$K_1'(y) = -K_0(y) - \frac{K_1(y)}{y},$$

whence

$$\left[K_1(y) + \varepsilon\left(-K_0(y) - \frac{K_1(y)}{y}\right)\right](y+\varepsilon) \leq \left(1 - \frac{1}{n}\right) yK_1(y),$$

which simplifies to

$$\varepsilon \geq \frac{K_1(y)}{nK_0(y)}, \tag{9}$$

i.e.,

$$\delta \geq \delta_c = \frac{K_1(y)}{\alpha n K_0(y)}.$$

The graph of $\alpha\delta_c$ is given in Figure 2.

Note that if $\varepsilon = \alpha\delta_c$ satisfies inequality (8), i.e., $Q(\varepsilon) \leq 1 - 1/n$, then $\alpha\delta \geq \alpha\delta_c$ satisfies $Q(\varepsilon) \leq 1 - 1/n$ for all δ.

This follows despite the fact that $K_1(y+\varepsilon)$ is monotone decreasing in ε, while $(y+\varepsilon)$ is monotone increasing in ε. The derivative of $(y+\varepsilon)\,K_1\,(y+\varepsilon)$ is $-(y+\varepsilon)\,K_0\,(y+\varepsilon)$, hence, $(y+\varepsilon)\,K_1\,(y+\varepsilon)$ is monotone decreasing in ε. Thus, $Q(\alpha\delta_c) \geq Q(\alpha\delta)$ since $\alpha\delta_c \leq \alpha\delta$ for all δ. Hence, $Q(\alpha\delta) \leq Q(\alpha\delta_c) \leq 1 - 1/n$ for all δ.

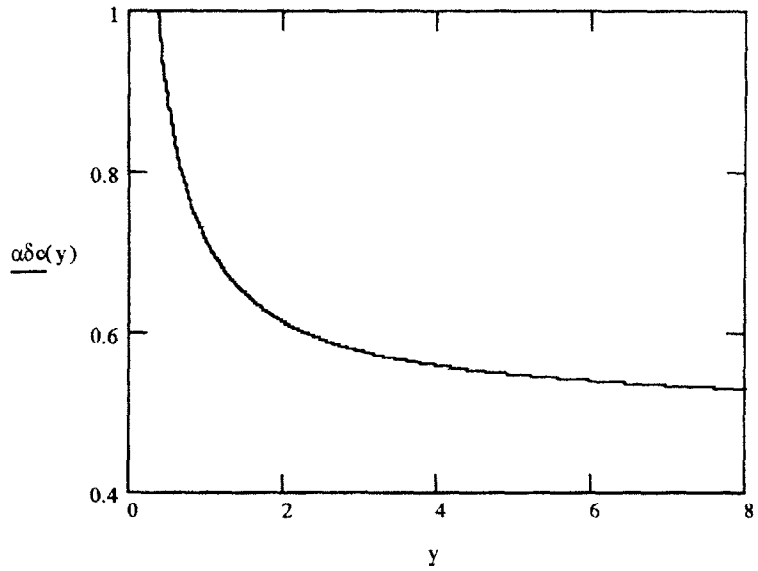

Figure 2. The graph of the width function $\varepsilon_c(y) = \alpha\delta_c(y)$, defined by inequality (9). In this graph $n = 2$.

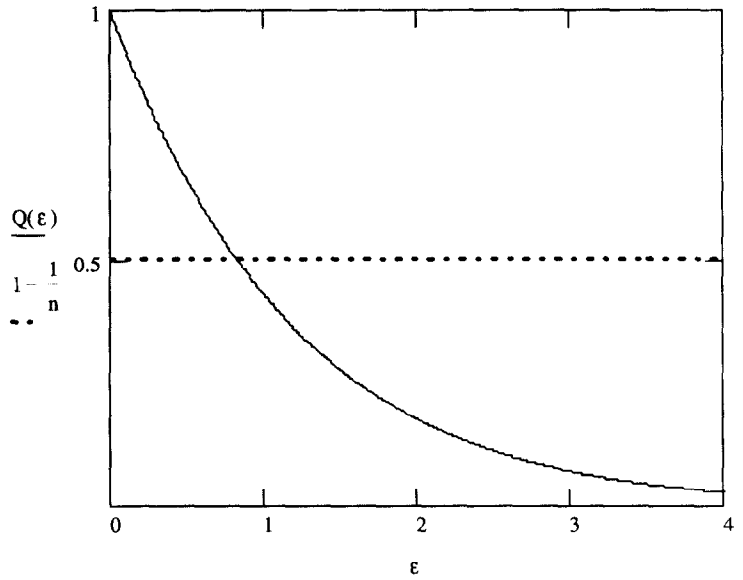

Figure 3. The graph of the function $Q(\varepsilon)$ defined by equation (8). The parameter values used are $y = 2$ and $n = 2$. The intersection of the dotted line with the graph of Q defines a minimum thickness of GF activity, below which no healing can occur.

Large values of n denote an active production rate which would certainly be necessary for healing. In Figure 3, the graph of $Q(\varepsilon)$ from equation (8) is illustrated for the parameter values $y = 2$ and $n = 2$.

A comparison of the values from the graph of equation (8) referred to as $(\alpha\delta_c)_g$ (with no approximation except rounding) and the values from equation (9) referred to as $\alpha\delta_c$ are given in Table 1.

Using this value of δ_c, a representative for R_c-values can be sought. Using equation (8), we can write

$$Q(y) = \frac{(y+\varepsilon)\,K_1(y+\varepsilon)}{yK_1(y)} \leq 1 - \frac{1}{n}. \tag{10}$$

Table 1.

n	$1-\frac{1}{n}$	αR	$\alpha\delta_c$	$(\alpha\delta_c)_g$	$(\alpha\delta_c)_g - \alpha\delta_c$
1.5	$.\overline{3}$	1	.95	1.39	.44
1.5	$.\overline{3}$	3	.77	1.22	.45
1.5	$.\overline{3}$	5	.73	1.15	.42
1.5	$.\overline{3}$	7	.71	1.16	.45
1.5	$.\overline{3}$	10	.70	1.16	.46
1.5	$.\overline{3}$	20	.68	1.13	.45
5.0	.8	1	.29	.307	.017
5.0	.8	3	.23	.253	.023
5.0	.8	5	.22	.244	.024
5.0	.8	7	.21	.235	.025
5.0	.8	10	.21	.235	.025
5.0	.8	20	.20	.226	.026
8.0	.9	1	.18	.190	.01
8.0	.9	3	.14	.154	.014
8.0	.9	5	.14	.145	.001
8.0	.9	7	.13	.145	.015
8.0	.9	10	.13	.140	.01
8.0	.9	20	.13	.137	.007

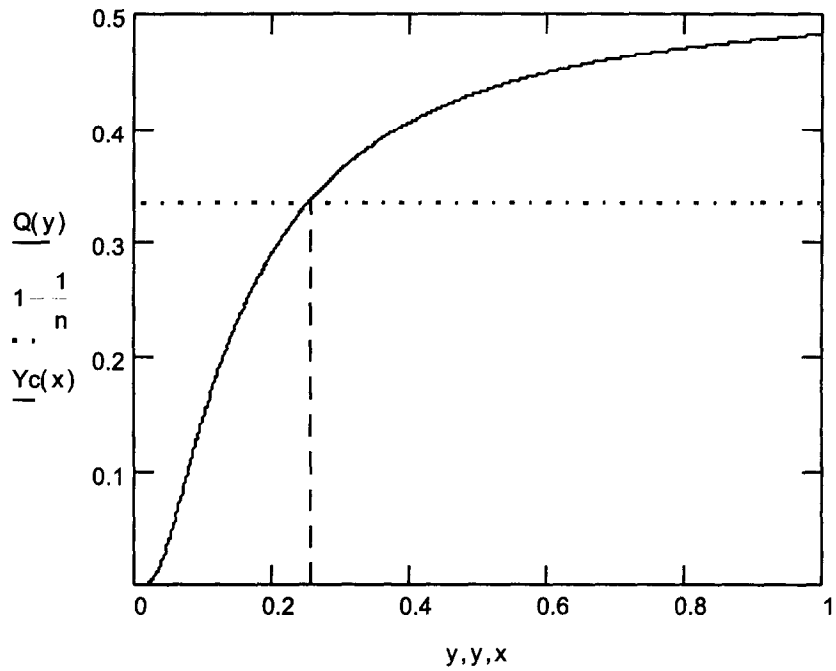

Figure 4. The graph of $Q(y)$ where the approximation $\varepsilon_c(y)$ replaces ε in $Q(\varepsilon)$. The resulting graph shows the region that satisfies the inequality; namely $(0, y_c]$; y_c is represented by the vertical line. n =1.5 was chosen for this illustration.

By substituting $(K_1(y))/(nK_0(y))$ for ε in equation (10) and simplifying the result, $Q(y)$ becomes

$$Q(y) = \left(\frac{nyK_0(y) + K_1(y)}{nyK_0(y)K_1(y)}\right) K_1\left(y + \frac{K_1(y)}{nK_0(y)}\right) \leq 1 - \frac{1}{n} \tag{11}$$

the graph of which is given in Figure 4.

The parameter value used for Figure 4 is $n = 1.5$.

Solving for y from equation (11) is not feasible, analytically, at least. However, observe that the graph of Figure 4 resembles that of a rational function. Thus, by finding a rational function which approximates $Q(y)$, it should be possible to approximate R_c by an explicit formula.

A rational function which approximates $Q(y)$ for various parameter values is

$$F(y) = b - \frac{a}{y}$$

for suitable a and b, both positive. Solving $b - a/y \leq 1 - 1/n$ for y, the formula for αR_c or y is

$$\alpha R \leq \alpha R_c = \frac{a}{b + 1/n - 1}.$$

In Figure 5, for $n = 1.5$

$$F(y) = .523 - \frac{.048}{y}$$

and $y \approx .253$ while graphical methods give $y \approx .252$.

Some additional comparisons are given in Table 2.

An interesting observation is that using the minimum value for $\alpha\delta_c$ will always produce a CSD because of the dependence on n in the equation. (See equation (11).) For n very large, e.g., $n = 200$, the graph of equation (11) is shown in Figure 6.

If we choose an $\alpha\delta > \alpha\delta_c$ such as $(\beta K_1(y))/(nK_0(y))$ for $\beta \geq 1$, it is possible to create graphs which show no CSD is possible. For example; for $n = 2$ and $\beta = 1$, 1.2, and n

$$Qi(y) = \left(\frac{nyK_0(y) + \beta K_1(y)}{nyK_0(y)K_1(y)}\right) K_1\left(y + \frac{\beta K_1(y)}{nK_0(y)}\right) \leq 1 - \frac{1}{n}, \qquad \text{for } i = 0, 1, 2, \tag{12}$$

(which is true from an earlier conjecture) graphs are given in Figure 7. Thus, using an $\alpha\delta$ value larger than the minimum might yield a situation modeling complete healing. For $\beta = 1$, $Q(y)$ represents $\alpha\delta_c$ substituted for ε. For $\beta = 1.2$, Q_1(y) represents a situation which shows the existence of a CSD. For $\beta = n$, $Q_2(y)$ is exhibiting a graph with no CSD.

MODEL II: EQUATIONS AND SOLUTIONS

In this model, as indicated above, there is still some tissue in the wound interior for $r < R$. It is merely a passive environment into which GF can diffuse. As before, the ring from the wound edge at R to $R + \delta$ is the domain of GF production. Additional boundary conditions need to be imposed, namely continuity of $C(r)$ and $(dC(r))/(dr)$ at R.

The corresponding solutions are

$$\begin{aligned}
C(r) &= AI_0(\alpha r) + BK_0(\alpha r), && \text{for } r < R,\\
C(r) &= MI_0(\alpha r) + NK_0(\alpha r) + \frac{P}{\lambda}, && \text{for } R \leq r \leq R + \delta,\\
C(r) &= GK_0(\alpha r), && \text{for } r > R + \delta.
\end{aligned}$$

Let $\beta = (I_0K_1 + K_0I_1)(\alpha r)$ and β_δ as before, then

$$C(r) = \frac{P}{\lambda}\left(\frac{K_1(\alpha R)}{\beta} - \frac{K_1(\alpha(R+\delta))}{\beta\delta}\right) I_0(\alpha r), \qquad \text{for } r < R, \tag{13}$$

$$\begin{aligned}
C(r) = {} & \frac{-P}{\lambda}\left(\frac{K_1(\alpha(R+\delta))}{\beta\delta}\right) I_0(\alpha r)\\
& + \frac{-P}{\lambda}\left(\frac{I_1(\alpha R)}{\beta}\right) K_0(\alpha r) + \frac{P}{\lambda}, \qquad \text{for } R \leq r \leq R + \delta,
\end{aligned} \tag{14}$$

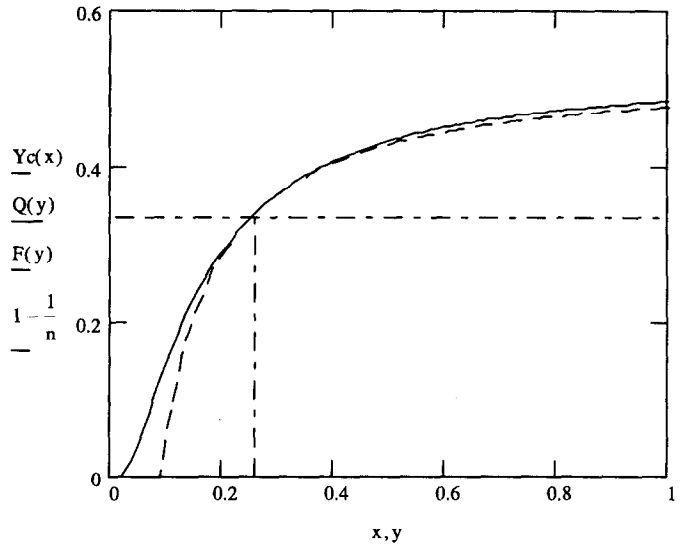

Figure 5. The graph of Figure 4 and its rational approximation $F(y)$. Ideally $F(y)$ attains its most accurate representation of $Q(y)$ in the vicinity of $y = 1 - 1/n$. As the value of n is changed new values for a and b must by found. For this graph $n = 1.5$, $a = .048$, and $b = .523$.

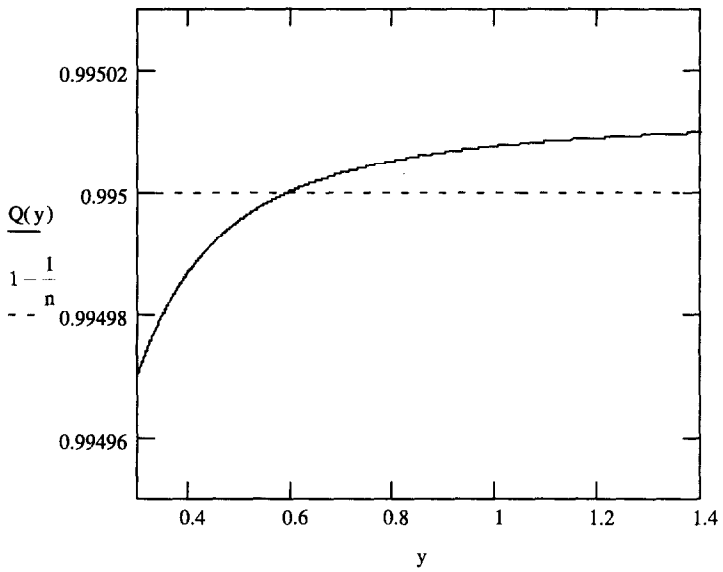

Figure 6. Figure 4 reproduced for n =200. The purpose of this graph is to illustrate the existence of a CSD no matter how large an n is chosen.

Table 2.

n	$1 - \frac{1}{n}$	$(\alpha R_c)_g$	αR_c	a	b
1.1	.091	.13	.155	.050	.413
1.5	.333	.26	.237	.045	.523
3.0	.667	.40	.480	.029	.727
5.0	.800	.45	.487	.014	.829
8.0	.875	.54	.572	.010	.892
10	.900	54	.539	.008	.915
20	.950	.59	.670	.002	.952

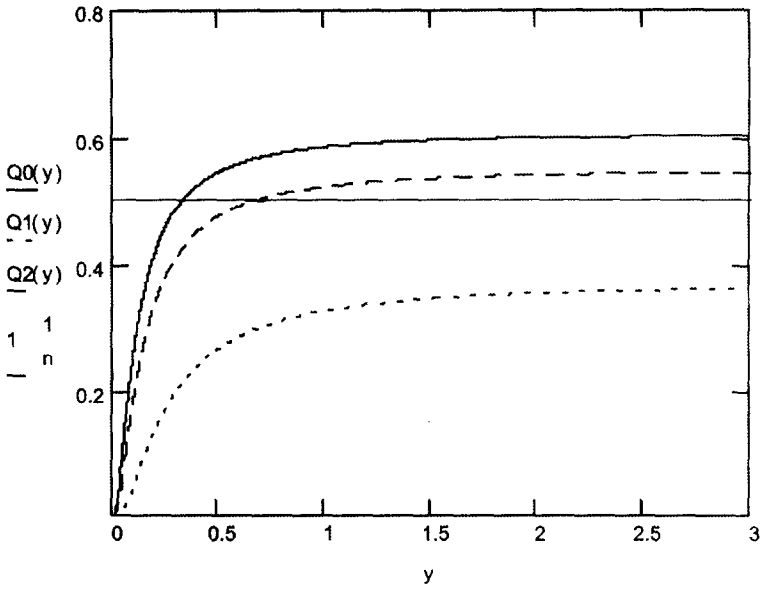

Figure 7. For $i = 0, 1, 2$ and $n = 2$ in equation (12), $Q_i(y) \geq \alpha\delta_c(y)$. For $i = 2$ complete healing occurs as observed by the graph of $Q_2(y)$. For $i = 1$, $Q_1(y)$ intersects $1 - 1/n$ which implies the exstence of a CSD. $Q_0(y) = \alpha\delta_c(y)$ (i.e., β =1). $Q_1(y)$ corresponds to $\beta = 1.2$ and $Q_2(y)$ corresponds to $\beta = 2$.

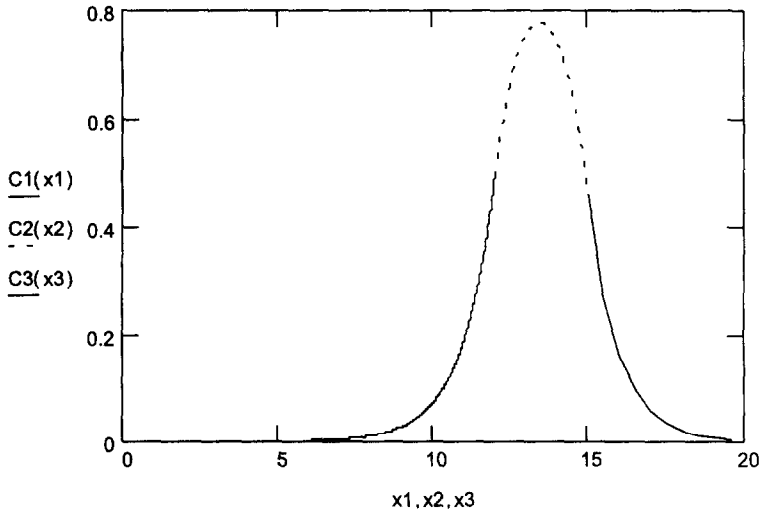

Figure 8. The growth factor concentration $C(r)$ for Model II, which assumes some bone is left in the wound area, $r \leq R$, where R is the radius size of the circular wound. $x1 = r$ for r in $[0, R]$, $x2 = r$ for r in $[R, R+\delta]$, and $x3 = r$ for r in $[R+\delta, \infty]$. For illustrative purposes, the parameters P and $\lambda = 1$, $\alpha R = 12$, and $\alpha\delta = 3$.

and

$$C(r) = \frac{-P}{\lambda}\left(\frac{I_1(\alpha R)}{\beta} - \frac{I_1(\alpha(R+\delta))}{\beta\delta}\right)K_0(\alpha r), \qquad \text{for } r > R + \delta. \tag{15}$$

A typical graph of $C(r)$ using parameter values P, $\lambda = 1$, $\alpha R = 12$, and $\alpha\delta = 3$ can be seen in Figure 8.

The requirement $C(R) \geq \theta$ implies, from equation (14) that

$$\alpha(R+\delta)K_1(\alpha(R+\delta))I_0(\alpha R) + \alpha R I_1(\alpha R)K_0(\alpha R) \leq 1 - \frac{1}{n}.$$

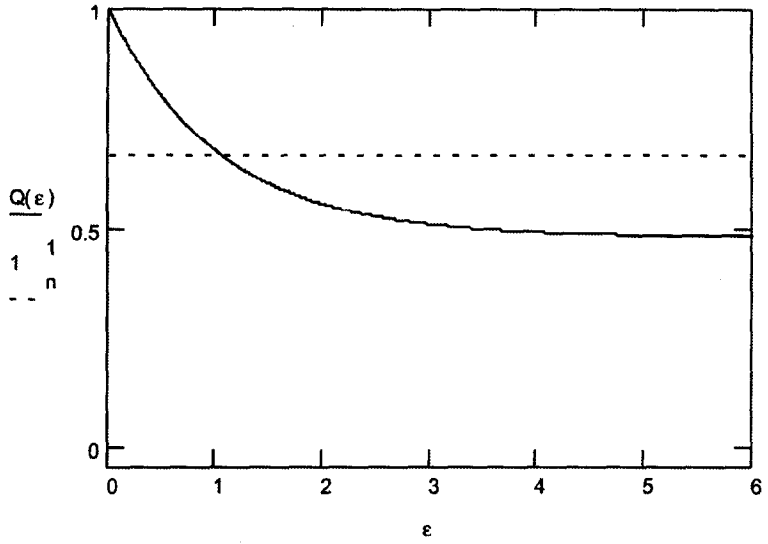

Figure 9. The graph represents the function $Q(\varepsilon) \leq 1 - 1/n$. The parameter values used are $y = 12$ and $n = 3$.

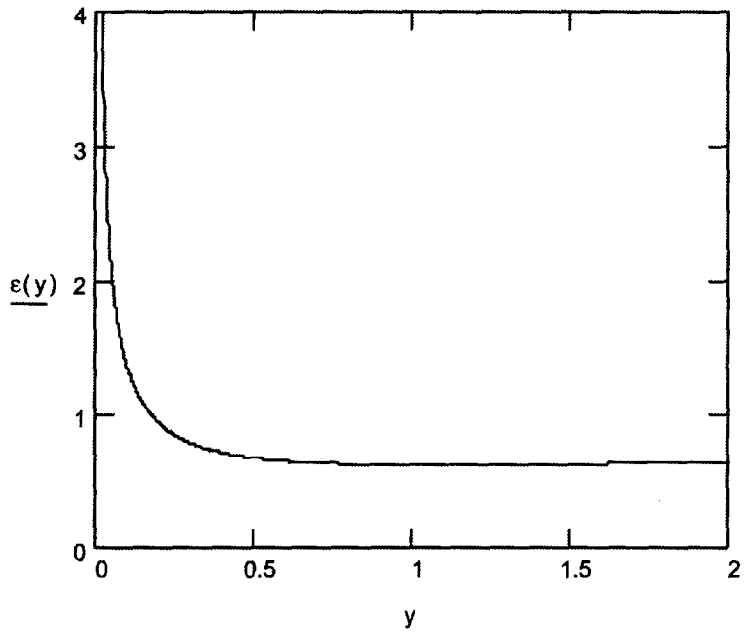

Figure 10. The graph of the approximation function $\varepsilon_c(y) = \alpha\delta_c(y)$. In this graph $n = 3$.

Again, if $\varepsilon = \alpha\delta$ and $y = \alpha R$, then this becomes

$$Q(\varepsilon) = (y + \varepsilon)K_1(y + \varepsilon)I_0(y) + yI_1(y)K_0(y) \leq 1 - \frac{1}{n}, \tag{16}$$

the graph of which is given in Figure 9, using parameter values $n = 3$ and $y = 12$.

By similar methods to those used in Model I, we can find an approximation for δ_c under the assumption that $\delta/R \ll 1$. This is

$$\delta \geq \delta_c = \frac{1}{n\alpha y K_0(y) I_0(y)}$$

or

$$\alpha\delta \geq \alpha\delta_c = \varepsilon_c(y) = \frac{1}{nyK_0(y)I_0(y)} \tag{17}$$

the graph of which is given in Figure 10 (for $n = 3$).

Again, substituting $\alpha\delta_c = \varepsilon_c(y)$ from equation (17) for ε in equation (16) we obtain the following graph (Figure 11) for the parameter value $n = 3$. The rational function $F(y)$ which closely approximates

$$Q(y) = \left(y + \frac{1}{nyK_0(y)I_0(y)}\right) K_1\left(y + \frac{1}{nyK_0(y)I_0(y)}\right) I_0(y) + yI_1(y)K_0(y) \leq 1 - \frac{1}{n}$$

with $n = 3$ is

$$F(y) = \frac{by}{c+y}, \qquad \text{for } b = .765 \text{ and } c = .059$$

(see Figure 12).

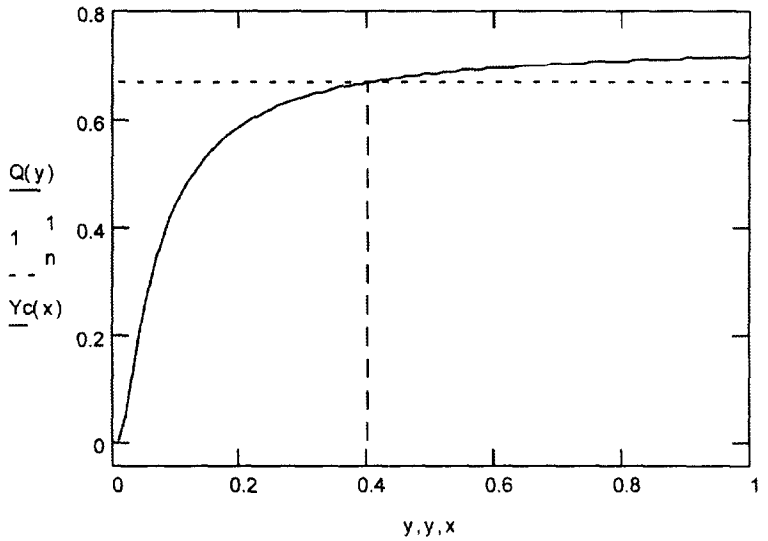

Figure 11. The graph of $Q(y) \leq 1 - (1/n)$, where the approximation $\varepsilon_c(y)$ replaces ε in equation (15). The resulting graph shows the region the satisfies the inequality namely $(0, y_c]$; y_c is represented by the vertical line. $n = 3$ was chosen for this illustration.

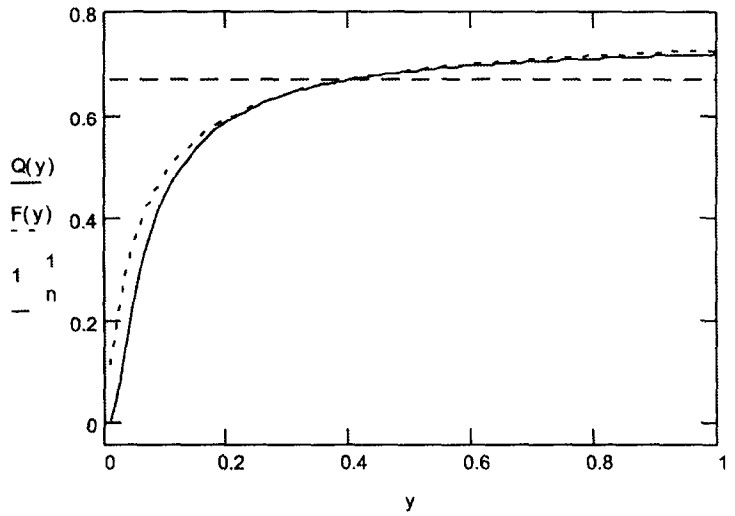

Figure 12. The graph of Figure 11 and its rational approximation $F(y)$. $F(y)$ attains its most accurate representation of $Q(y)$ in the vicinity of $y = 1 - 1/n$. As the value of n is changed new values for b and c must be found. For this graph $n = 3$, $b = .765$, and $c = .059$.

Table 3.

n	$1-\frac{1}{n}$	αR	$\alpha\delta_c$	$(\alpha\delta_c)_g$	$(\alpha\delta_c)_g - \alpha\delta_c$
1.5	$.\overline{3}$	1	1.251	2.58	1.329
1.5	$.\overline{3}$	3	1.311	none	
1.5	$.\overline{3}$	5	1.326	none	
1.5	$.\overline{3}$	7	1.330	none	
1.5	$.\overline{3}$	10	1.332	none	
1.5	$.\overline{3}$	20	1.333	none	
5.0	.8	1	.3750	.400	.025
5.0	.8	3	.3930	.470	.077
5.0	.8	5	.3980	.490	.092
5.0	.8	7	.3990	.500	.101
5.0	.8	10	.3990	.500	.101
5.0	.8	20	.3990	.500	.101
8.0	.9	1	.2340	.250	.016
8.0	.9	3	.2460	.270	.024
8.0	.9	5	.2490	.280	.031
8.0	.9	7	.2490	.280	.031
8.0	.9	10	.2500	.280	.230
8.0	.9	11	.2500	.290	.040

Table 4.

n	$1-\frac{1}{n}$	$(\alpha R_c)_g$	αR_c	b	c
1.1	.091	.116	.072	.597	.4
1.5	.333	.237	.240	.639	.22
3.0	.667	.400	.450	.755	.06
5.0	.800	.480	.466	.845	.026
8.0	.875	.510	.543	.899	.015
10	.900	.530	.585	.909	.006
20	.950	.560	.598	.952	.0015

The explicit formula for y from $by/(c+y) \leq 1-(1/n)$ is

$$y = \frac{c - cn}{n - 1 - bn}. \tag{18}$$

(In Table 3 where the $(\alpha\delta_c)_g$ values from the graph show none, the entire graph lay above $1-(1/n)$.)

Tables 3 and 4 show some values for $\alpha\delta_c$ and αR_c that were found for Model II in the same manner as that of Model I.

RELEVANT EXPERIMENTAL DETAILS

Many experiments on wound healing have been done on rats, rabbits, and dogs, but not much literature has been written on experiments for monkeys or humans. From the literature which we do have, the wound was created in the calvaria, which is the bony part of the cranium from the base of the skull to the forehead. In [6], Prolo implies that humans do not react the same as other animals to calvaria wounds because of a poorer blood supply in the calvaria and some deficiency of bone marrow. This seems to imply that the experiments on the lower mammals may not extend in the same manner to humans. Freeman and Turnbull [7,8] were the first to attempt the study of CSDs in rat calvaria. In a 500 mg Wilstar albino rat they studied a 2 mm-diameter CSD, which failed to heal in 12 weeks. Mulliken and Glowacki [9] and Glowacki *et al.*

[10] found 4 mm-diameter to be the CSD in young (28 days old) Charles River rats. Tagaki and Urist [5] found 8 mm-diameter to be the CSD in six month old Sprague-Dawley rats. It did reduce to 5 mm-diameter in four weeks, but no further healing was noticed at the end of 12 weeks. Kramer *et al.* [11] experimented on the calvaria of 6 to 10 pound New Zealand White rabbits. They found 8 mm-diameter CSDs occurred at various periods up to 16 weeks. Frame [12] worked with a crossbreed of New Zealand White and Half Lop rabbits. He made 5, 10, 15, and 20 mm-diameter wounds in the calvaria of these 6.6 to 10.5 pound rabbits. At 24 and 36 weeks, the 15 mm-diameter wound had created the fibrous connective tissue but continued to retain a central uncalcified area. Friedenberg and Lawrence [13] described the wound healing experiments with mongrel dogs. A 17 mm-diameter had less than 40% osseous repair at 20 weeks. Prolo *et al.* [14] found that a 20 mm-diameter in mongrel dogs healed 20% by six months. Urist [15] also suggested that 20 mm-diameter was a reasonable CSD in dogs. These experiments show us that there is a critical size defect, in the general range of 2 mm–2 cm. We might also conclude that monkeys and humans will probably have a CSD larger than 2 cm. (Values for α are in the range of $.05\,\mathrm{cm}^{-1}$ to $6\,\mathrm{cm}^{-1}$.)

CONCLUSIONS

When a bone wound occurs, the body produces electrical signals that stimulate growth hormones in the bone. These growth hormones, which we have called growth factors, trigger the natural healing process. For reasons which are poorly understood, sometimes bone wounds fail to heal properly (these are called nonunions). Our mathematical model demonstrates why this may occur. Obviously there are many factors affecting these nonunions, but some of the most logical observations in humans are that adults do not heal as well as the young, and adults, who may have other health challenges, may be unable to heal completely [16]. The mathematical model indicates that there exists a lower bound value for the width of the growth hormone region, and if that width is no less than this value then the GF concentration is such that healing may ensue. This by itself does not ensure complete healing, but that some healing will occur. In this model, we have shown the dependence of the GF region on the original size of the wound. Obviously, this region is limited in size by the animal and by the size of the region in the calvaria available to stimulate the GF region. Wounds that are too large may not have enough GF to stimulate complete healing, (i.e., $C(R) < \theta$). It may also be the case, that $C(R) \geq \theta$ but due to the long time (several weeks to years) needed to complete the healing process, the GF region may not be adequate in size. According to both Models I and II, sufficiently large wounds do not have enough GF in proximity to the wound center and to the edge to stimulate and maintain healing growth, and thus, complete the healing process. This creates the CSD.

In earlier work [1], a value for α was estimated from entirely phenomenological considerations for illustrative purposes. The basis for this estimate was soft tissue data, and yielded $\alpha \approx 6\,\mathrm{cm}^{-1}$. Clearly, the CSD phenomenon is confined to bone, and it is reasonable to ask what range of α-values might be appropriate. Since $\alpha = \sqrt{\lambda/D}$ this is equivalent to asking how both λ and D change from soft to hard tissue environments. Unfortunately, this data, if known at all, is difficult to come by. The best that can be done at this stage is to make some plausible estimates of their orders of magnitude.

Diffusion processes alone will not suffice in bone to provide nourishment for the osteocytes, but capillaries are never far away: the osteocytes are arranged around central capillaries in concentric layers, which form spindle-shaped units known as osteons. Thus, pure diffusion is facilitated by the efficient capillary transport system, and we might expect that the *effective* diffusion coefficient is enhanced compared with the standard value used in [1] (at least for growth factors of the same molecular weight). Concerning the decay coefficient λ it is even harder to speculate. Given the increased average density of bone compared with soft tissue, the effective decay of GF *may* be hindered somewhat (i.e., λ reduced). It is difficult to be more precise at this stage, but again, for

the purposes of illustration, we suppose that, compared with the values used in [1], λ is *halved* and D is increased by a factor of five. Thus, we take $\lambda \approx 8 \times 10^{-6}\,\mathrm{sec}^{-1}$ and $D \approx 2.5 \times 10^{-6}\,\mathrm{cm}^2\,\mathrm{sec}^{-1}$. This results in a value of $\alpha \approx 1.8\,\mathrm{cm}^{-1}$. It can be seen from Column 4 in Table 2, and 4 in this paper, that the dimensionless quantity αR_c ranges from about 0.07 to 0.95; for the above value of α this corresponds to R_c in the range 0.4 mm to 5.3 mm which is certainly of the right order of magnitude for the lower end of the CSD sizes quoted above corresponding to a diameter range of 1 mm–1 cm. It must be emphasized however, that our values for α are only as valid as the values for λ and D, and these are estimated. Clearly, quantitative validation of the consistency of the models in this paper, must await measurement of these parameters based on experimental data.

(A subsequent paper will address the three-dimensional problem, this is more appropriate in the context of, for example, surgical excision.)

REFERENCES

1. J.A. Adam, A simplified model of wound healing (with particular reference to the critical size defect), *Mathl. Comput. Modelling* **30** (5/6), 23–32, (1999).
2. EBI Medical Systems, EBI Bone healing Systems: Internet `www.ebimedical.com/normal_boneheal.html`.
3. J.A. Sherratt and J.D. Murray, Models of epidermal wound healing, *Proc. R. Soc. Lond.* **241B**, 29–36, (1990).
4. J.A. Sherratt and J.D. Murray, Mathematical analysis of a basic model for epidermal wound healing, *J. Math. Biol.* **29**, 389–4044, (1991).
5. C.J. Tranter, *Bessel Functions With Some Physical Applications*, Hart Publishing, New York, (1969).
6. D.J. Prolo, P.W. Pedrotti, K.P. Burres and S. Oklund, Superior osteogenesis in transplanted allogenic canine skull following chemical sterilization, *Clin. Orthrop.* **108**, 230, (1982).
7. E. Freeman and R.S. Turnbull, The role of osseous coagulum as a graft material, *J. Periodont. Res.* **8**, 229, (1973).
8. R.S. Turnbull and E. Freeman, Use of wounds in the parietal bone of the rat for evaluating bone marrow for grafting into periodontal defects, *J. Periodont. Res.* **9**, 39, (1974).
9. J.B. Mulliken and J. Glowacki, Induced osteogenesis for repair and construction in the craniofacial region, *Plast. Reconstr. Surg.* **65**, 553, (1980).
10. J. Glowacki, D. Altobelli and J.B. Mulliken, Fate of mineralized and demineralized osseous implants in cranial defects, *Cacif. Tissue Int.* **33**, 71, (1981).
11. I.R.H. Kramer, H.C. Kelly and H.C. Wright, A histologicaland radiological comparison of the healing of defects of the rabbit calvarium with and without implanted heterogenous anorganic bone, *Arch. Oral Biol.* **13**, 1095, (1968).
12. J.W. Frame, A convenient animal model for testing bone substitute materials, *J. Oral Surg.* **38**, 176, (1980).
13. Z.B. Friedenberg and R.R. Lawrence, *Surg. Gynecol. Obstet.* **114**, 721, (1962).
14. M.R. Urist, New advances in bone research, *West. J. Med.* **141**, 71, (1984).
15. Fractures Treatment methods are tailored to the break, Mayo Clinic Health Letter, Internet `www.mayohealth.org/mayo/9604/htm/fracture.htm`, (1986).
16. F. Bowman, *Introduction To Bessel Functions*, Dover Publications, New York, (1958).
17. L. Du Noüy, *Cicatrization Of Wounds (II)—Experimental Technique-Curves-Mathematical Study*, Methuen, London, (1936).
18. J.W. Frame, A composite of porous calcium sulfate dihydrate and cyanoacrylate as a substitute for autogenous bone, *J. Oral Surg.* **38**, 251, (1980).
19. R.W. Ruddon, *Cancer Biology*, Second Edition, Oxford University, New York, (1987).
20. J.P. Schmitz and J.O. Hollinger, The critical size defect as an experimental model for craniomandibulofacial nonunions, *Clinical Orthopaedics and Related Research* **205**, 299–308, (1986).
21. K. Takagi and M.R. Urist, The reaction of the dura to Bone Morphogenetic Protein (BMP) in repair of skull defects, *Ann. Surg.* **196**, 100, (1982).